Pressure-Volume-Temperature of molten and glassy polymers

Utracki, L. A.

Publisher's version / Version de l'éditeur:
https://doi.org/10.1002/polb.21031
Journal of Polymer Science Part B: Polymer Physics, 45, 3, pp. 270-285, 2007-02-01

Pressure–Volume–Temperature of Molten and Glassy Polymers

L. A. UTRACKI

Industrial Materials Institute, National Research Council, Canada, 75 de Mortagne, Boucherville, Quebec J4B 6Y4, Canada

Received 24 August 2006; revised 28 September 2006; accepted 28 September 2006
DOI: 10.1002/polb.21031
Published online in Wiley InterScience (www.interscience.wiley.com).

ABSTRACT: The pressure–volume–temperature (*PVT*) dependencies of several amorphous polymers (PS, PC, PPE, and PPE/PS 1:1 blend) in the glassy and molten state were studied. The Simha–Somcynsky (*S*–S) lattice-hole equation of state (EOS) was used. Fitting the *PVT* data in the molten state to the EOS yielded the free volume quantity, $h = h(T, P)$, and the characteristic reducing parameters, P^*, V^*, and T^*. The data within the glassy region were interpreted assuming that the latter parameters are valid in the molten and vitreous state, than calculating $h = h(T, P)$ from the experimental values of $V = V(T, P)$. Next, the frozen free volume fraction in the glass was computed as $FF = FF(P)$. The *FF* values of polystyrene (PS) resins at ambient pressure showed little scattering ($FF_{P=1} = 0.691 \pm 0.008$), while their *P*-dependencies varied, reflecting the thermodynamic history of the glass formation as well as the *PVT* measurements protocol. The pressure gradient of T_g was compared with the Ehrenfest relation for the second-order transition; here also agreement depended on the method of vitrification. The experimental values of *FF* at ambient pressure decreased with increasing values of the characteristic temperature reducing parameter, T^*. ©2006 Wiley Periodicals, Inc. J Polym Sci Part B: Polym Phys 45: 270–285, 2007

Keywords: equation-of-state; free volume; glass transition; phase behavior; statistical thermodynamics; thermodynamics; vitreous state behavior

INTRODUCTION

The pressure–volume–temperature (*PVT*) dependence of polymers has been measured primarily to determine compressibility, κ, and the thermal expansion coefficient, α, the parameters essential in polymer engineering:

$$\kappa \equiv -\left(\frac{\partial \ln V}{\partial P}\right)_{T,P^o,q}; \alpha \equiv \left(\frac{\partial \ln V}{\partial T}\right)_{T^o,P,q} \quad (1)$$

Here P^o and T^o are the glass formation pressure and temperature, respectively. In the glassy state, the two relations depend on *P*, *T*, the vitrification procedure, and the rate of heating or compressing, *q*. For polymer melts, within narrow ranges of *T* and *P*, the rate *q* is relatively slow (compared with molecular relaxations), and the customary definitions for κ and α specify only one variable: *T* or *P*, respectively.

For the molten state, several equations of state (EOS) have been proposed.[1–8] Furthermore, the Tait empirical relation for seawater density also has been used.[9] Curro,[10] Zoller,[11] Rodgers,[12] and Rudolf et al.[13] reviewed and evaluated the suitability of several EOS to describe the *PVT* surface within the liquid state. The Simha–Somcynsky (*S*–S) theory[4] was found to well describe the *PVT* dependencies,[14–18] as well as to provide good measure of the internal pressure, surface tension, cohesive energy density, or solubility parameters.[19,20] The *S*–S EOS is unique by explicit incorporation of the free volume parameter, *h*, used for

Correspondence to: L. A. Utracki (E-mail: leszek.utracki@cnrc-nrc.gc.ca)

Journal of Polymer Science: Part B: Polymer Physics, Vol. 45, 270–285 (2007)

interpretation of nonequilibrium properties such as the kinetics of volume relaxation,[21] flow behavior,[22–25] or positron annihilation lifetime spectroscopy (PALS).[26–31]

Formally, the passage from the molten to glassy state involves Ehrenfest second-order phase transition for constant formation of glass:[32]

$$\frac{dT_g}{dP} = \frac{\Delta\kappa}{\Delta\alpha}; \quad or \quad \frac{dT_g}{dP} \cong \left(\frac{\partial T}{\partial P}\right)_{h,l} \tag{2}$$

where Δ specifies a difference between values for the liquid and glassy state, and subscript "l" indicates liquid state. The relation is supposed to be automatically valid if proper κ-values are used.[33] The validity was confirmed for glasses prepared under ambient pressure, but not for those prepared at high P.[34]

Rigorous theoretical analyses of polymer *PVT* behavior in vitreous state have rarely been carried out—the main reason being inadequate theoretical description of the thermodynamic history and time dependent glass structures.[35]

Arora et al.[36] modified the cell model of Prigogine et al.[1,2] with the Lennard-Jones (L-J) interactions,[37] without the usual assumption of the square-well potential (SWP):

$$\tilde{P}\tilde{V}/\tilde{T} = 1 + (4/\tilde{T})[F_L/\tilde{V}^4 - F_M/\tilde{V}^2] + (2/\tilde{T})[A/\tilde{V}^4 - B/\tilde{V}^2] \tag{3}$$

The reduced variables are defined in terms of the L-J maximum attractive energy, ε^*, and the segmental repulsion volume, v^*, per statistical segment, the latter defined as $M_s = M_n/s$, where M_n is the number-average molecular weight, and s is the number of macromolecular segments.

$$\left.\begin{aligned} \tilde{P} &= P/P^*; \quad P^* = zq\varepsilon^*/(sv^*) \\ \tilde{T} &= T/T^*; \quad T^* = zq\varepsilon^*/(Rc) \\ \tilde{V} &= V/V^*; \quad V^* = v^*/M_s \end{aligned}\right\} (P^*V^*/T^*)M_s = Rc/s \tag{4}$$

In eq 3 the parameters $A = 1.011$ and $B = 1.2045$ are for the face-centered cubic lattice, and the integrals F_L and F_M are tabulated in ref. 36. In eq 4 the additional quantities are $3c$ (the external, volume-dependent degrees of freedom), $zq = s(z - 2) + 2$ (the number of interchain contacts in a lattice of the coordination number $z = 12$), and R (the gas constant).

Equation 3 describes the behavior of condensed systems, in which the free volume fraction $h \to 0$. Numerically, at $P \to 0$, it follows the relation originally proposed for liquids, but with different values of the two numerical parameters, $a = -0.0752$ and $b = 7.956$:[38]

$$\ln \tilde{V} = a + b\tilde{T}^{3/2} \tag{5}$$

Following the example of Arora et al., Sachdev and Jain analyzed the *PVT* behavior of high-density polyethylene (HDPE), distinguishing molten, semicrystalline, and crystalline state, each with its own set of P^*, V^*, T^*.[39] The implication of discontinuity in the Lennard-Jones (L-J) potential is inconsistent with the fundamental concepts of physics, and therefore an alternative concept must be used.

The *S*–S lattice-hole theory was derived for the liquid state.[4] The model lattice contains volume fraction y of occupied sites and the free volume (holes) fraction, $h = 1 - y$. Using the customary thermodynamic definition of pressure as $\tilde{P} = (\partial\tilde{F}/\partial\tilde{V})_{\tilde{T}}$ *S*–S obtained:

$$\tilde{P}\tilde{V}/\tilde{T} = (1 - U)^{-1} + 2yQ^2(AQ^2 - B)/\tilde{T} \tag{6}$$

where $Q = 1/(y\tilde{V})$, and $U = 2^{-1/6}yQ^{1/3}$ [assuming $y = 1$ and accepting the SWP reduces eqs 6–3]. Furthermore, for liquids at the thermodynamic equilibrium, minimization of the Helmholtz free energy with the free volume parameter h, $(\partial\tilde{F}/\partial h)_{\tilde{V},\tilde{T}} = 0$, leads to:

$$3c[(U - 1/3)/(1 - U) - yQ^2(3AQ^2 - 2B)/6\tilde{T}] + (1 - s) - (s/y)\ln[(1 - y) = 0 \tag{7}$$

The coupled eqs 6 and 7 describe the *PVT* liquid surface, and associated with it the free volume dependence, $h = h(\tilde{V}, \tilde{T})$. Fitting these relations to *PVT* data leads to a set of P^*, T^*, and V^* parameters, related to the L-J quantities, ε^* and v^*, through eq 4.

Considering the fundamental nature, precision, and wide applicability of the *S*–S theory, the following text will explore its applicability to melt and glass within the full range of experimentally accessible independent variables. The aim of this study is to analyze the *PVT* relations of amorphous polymers in the molten and glassy regions. Since the former one has been extensively discussed in the past, the glass transition and the vitreous state are of main interest.

GLASS TRANSITION AND THE GLASSY STATE

The glass transition is a process in which molten polymer is transformed into glass or *vice versa*.

Upon heating a glass at the glass transition temperature (T_g), the thermal energy overcomes the forces limiting large-scale segmental motions so that it may be transformed into liquid or elastomer. Phenomenologically, T_g marks freezing–unfreezing temperature of micro-Brownian motion involving 20–50 carbon atoms.[40]

If T_g is considered the main α-transition in amorphous polymers, there are secondary ones in the glassy and molten states. For the studied polymers, these secondary transitions, T_β and T_c, are usually too weak to affect the *PVT* surface, but they may become evident in derivative and/or spectroscopic quantities.

Thus, at $T < T_g$ immobile clusters and mobile defects dominate the material;[41] these are responsible for the glass–glass transitions, of which the β-transition, T_β, is closest to T_g, and it might affect the *PVT* behavior within the usual range of independent variables above the ambient conditions. For example, for PS T_β = 300–330,[42] for PPE $T_\beta \cong 367$, and for PC T_β = 166–185 K.[43–45] For most polymers the β-transition occurs at $T_\beta \approx 0.75 \times T_g$.[40]

Similarly at $T > T_g$, the melt is subjected to several relaxation processes, which result in secondary transitions. Of these the crossover temperature, $T_c/T_g \approx 1.25 \pm 0.05$, is the easiest to detect. At $T < T_c$ the α-relaxation of cages dominates, and at $T > T_c$ vibrations of molecular units in cages (from which they might escape) are dominant, and a true melt behavior might be observed.[46,47]

Glass formation depends on the way glass was prepared; thus, on the cooling or compressing rate, q, on the P during the cooling or T during the compressing, etc. Each glass-forming substance has a spectrum of states with different structures and the physical aging kinetics.[48] Virtually any material can be vitrified using an appropriate procedure, e.g., suitable cooling rate, for amorphous polymers $q \approx 0.01$, for metals at $q \approx 10^5$, while for noble gases (molecular dynamics data) at $q \approx 10^{12}$ K/s.

Several theories of glass transition have been proposed.[49–52] The thermodynamic theories consider the glass transition to be rate-affected second order; the glass is considered to exist in a pseudoequilibrium state. Furthermore, it is assumed that the free energy in glass must in time reach its minimum value. Nieuwenhuizen proposed to describe the thermodynamics of glass by using an additional entropy term related to slow configurational processes, which vanishes at equilibrium.[33]

The kinetic theories note that the glass transition strongly depends on the rate of cooling. For example, the pseudoequilibrium T_g values of polymers (tabulated in handbooks) are supposed to be measured at $q \leq 0.01$ K/s, or extrapolated to T at which the viscosity $\eta \approx 10^{12}$ Pa. However, with decreasing cooling rates the T_g decreases all the way to the Kauzmann zero-entropy temperature,[53] $T_K \approx T_g - 50\ \text{K} \approx T_0$, the latter parameter being the Vogel–Tammann–Fulcher temperature, defined in the relation:

$$\eta(T) = a_0 \exp\left\{\frac{a_1}{R(T - T_0)}\right\} \tag{8}$$

where a_0 and a_1 are equation constants.

As illustrated in Figures 1 and 2, T_g might be determined from the *PVT* plots either as the temperature at which straight lines drawn through ln V versus T isobaric dependencies intersect, or as the lowest temperature at which the ln V versus T^n ($n \leq 3/2$; $T > T_g$) relation remains linear. In the isobarically heated PS-667, T_g increases linearly with P at a slope of $dT_g/dP = 29.3$ (K/kbar), in good agreement with older data, $dT_g/dP \approx 30$ (K/kbar).[54] Similar values, 26.5 and 25 (K/kbar), were reported for polyvinyl acetate (PVAc)[55,56] and styrene-*co*-acrylonitrile (AN content ranging from about 5–40 wt %) (SAN),[35] respectively.

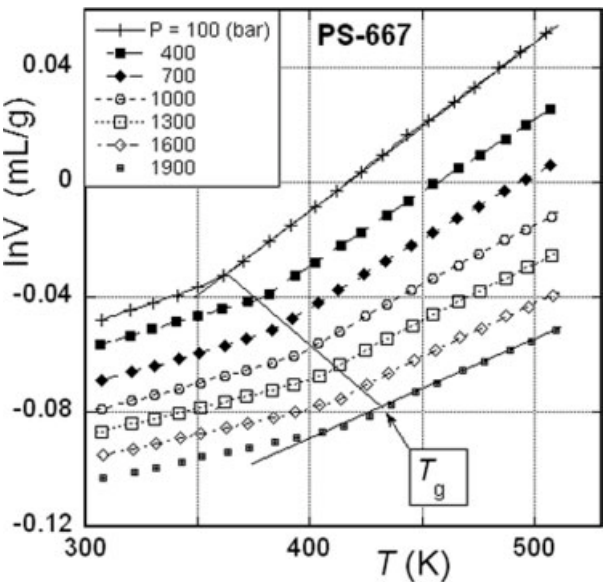

Figure 1. *PVT* diagram for PS-667 at 30–240 °C and P = 10–190 MPa. The extrudate was directly loaded and tested. Pressure linearly increases T_g. For the resin at P = 1 bar the secondary transitions at $T_\beta \cong 328$, and $T_c \cong 449$ K might be expected.

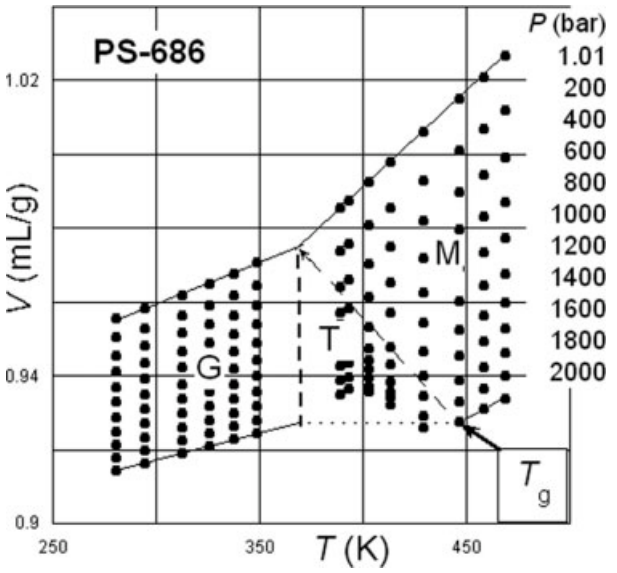

Figure 2. *PVT* diagram for PS-686 at 280–470 K and $P = 0.1$–200 MPa. The three symbols G, T, and M indicate the regions of glass, transient, and melt, respectively.

The regular V versus T behavior displayed in Figure 1 is to be compared with that shown in Figure 2. In the latter case, the specimen was also measured isobarically, but by cooling from the highest T. Strong cooling rate (or entropy change) related behavior was observed within the transition zone, **T**, immediately below T_g; in this case the initial pressure gradient, $dT_g/dP|_{P\to 0} \cong 48$ (K/kbar), slightly decreasing with P (see Fig. 4).

There have been several attempts to establish a simple predictive relation for T_g, *viz*. constancy ratio of T_g to the melting point, T_m; constant value of the reduced glass transition temperature, $\tilde{T}_g = T_g/T^*$; or constancy of the free volume fraction at T_g: $h_g = \text{const}$. At ambient pressure, these measures may provide a rough estimate of T_g (*e.g.*, $T_g/T_m = 0.66 \pm 0.11$,[57] $\tilde{T}_g = 0.0303 \pm 0.0041$ and $h_g = 0.070 \pm 0.018$), but the cited ranges are not random. For example, in Figure 3 h_g increases with T_g; a similar dependence was reported for $\tilde{T}_g = f(T_g)$,[38] while the ratio T_g/T_m is known to depend on maximum crystalline fraction.[52] Figure 3 also shows that the proposed simple relation is inadequate for higher pressures; as shown in Figure 4, the pressure increases T_g and decreases h_g. Gradients of these changes depend on the characteristic L-J interaction parameters of the polymer.

EXPERIMENTAL

Ten amorphous polymers listed in Table 1 were examined. The first on the list, PS-686, was measured by isobarically cooling the melt from about $T_g + 30$ °C, remelting it at the same temperature, increasing P (in steps of 200 bar from ambient up to 2000 bar) and step-wise cooling at a rate of 10 °C/min to the next level of T. The volume change

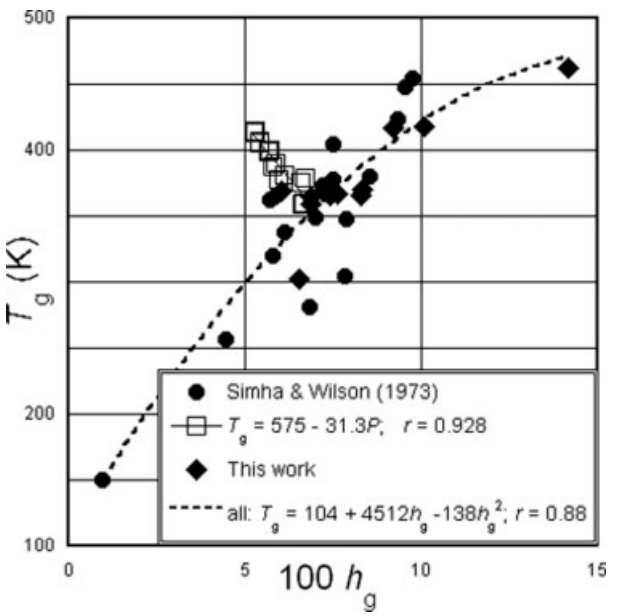

Figure 3. Glass transition temperature *versus* hole fraction for several polymers at $P = 0$ (circles) and for polymer evaluated in this work (diamonds).[38] The P-dependence for PS-667 at $P \leq 190$ MPa is indicated by open squares.

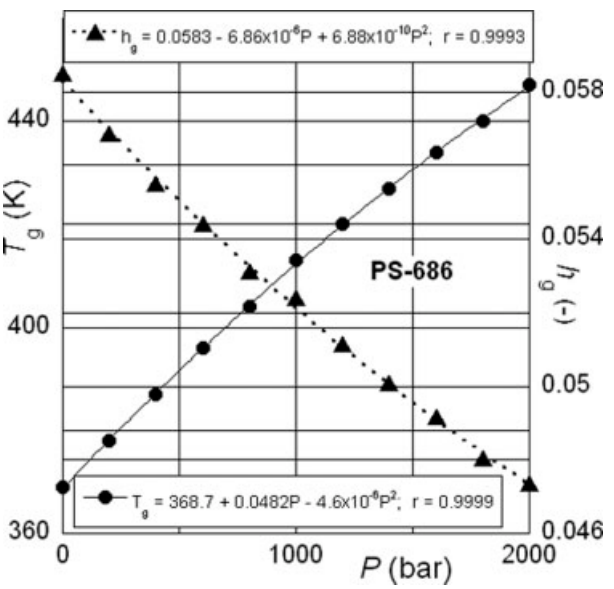

Figure 4. Pressure dependence of the glass transition temperature (solid circles) and hole fraction (solid triangles) for PS-686. The least squares fitting relations are also shown (see Table 3).

Table 1. Polymers Studied in This Work

No.	Polymer	Manufacturer	M_w (kg/mol)	M_n (kg/mol)	Ref.
1	PS-686	Dow Chemicals	279	90.7	34
2	PS-667[a]	Dow Chemicals	215	–	60
3	PS-1301	Nova Chemicals	270	–	17
4	PS-Z110	Polyscience	110	104	59
5	PS-Z34	Polyscience	34.5	32.6	59
6	PS-Z9	Polyscience	9.5	9.0	59
7	PS-Z09	Scientific Polymer Products	0.91	0.78	59
8	PC	General Electric	18.6	8.97	59
9	PPE	General Electric	244	32	59
10	PPE/PS = 1/1	Ref. No. D5096	179	–	59

[a] PS-667 contains 700 ppm Zn-stearate and 2.5% of mineral oil.

was read after thermal stabilization of ~2 h.[34,60] The results are displayed in Figure 2.

The extruded pellets of PS-677 were measured without premolding or annealing. The specimens were heated isobarically from ambient T to 240 °C in 170 T-steps at each level of P (instead of the usual 21), each step taking about 25 min (see Fig. 1). After the maximum temperature was reached, the sample was cooled, the pressure was increased by 300 bars, and then the next isobaric heating step commenced.

The remaining resins were tested after premolding either externally[59] or within the high-pressure dilatometer at $T \geq T_g + 30$ °C, and then cooling to room temperature at a rate of ~1 °C/min. The premolded specimens were tested isothermally, starting at the lowest T and P. At each T-level the pressure was increased from ca. 100 to 2000 bars in steps of 200 or 300 bars. The T was increased from room temperature in steps of about 10 °C (small effects of adiabatic heating were observed). This procedure is considered "standard" for the generation of *PVT* data. Its advantage is that the specimen sees the highest temperature only at the end of the test; thus, the measurements are not affected by thermal degradation.

Excepting PS-686 (studied in a specially constructed bellows dilatometer) the data were obtained using Gnomix™—a commercial, high-pressure dilatometer from Gnomix, Boulder, CO.[59] Only PS-686 and PS-667 were measured isobarically; the other tests followed the standard protocol. To examine data accuracy, the tests were repeated and effects of the holding time (from 0 to 90 s) were examined. The total run time was 18–32 h. The average error of measurements for specific volume was ≤0.03%. The *PVT* plots in Figures 1 and 2 show the limiting behaviors of amorphous polymers. The range of the independent variables usually extended from below T_β to above T_c, but these transitions were not observed on the standard *PVT* graphs of, for example, ln V versus T.

CALCULATIONS

The analysis of *PVT* behavior proceeded in three steps:

1. Molten state: Determination of the characteristic reducing parameters, P^*, T^*, V^*, and the free volume function, $h = h(V, T)$.
2. Glass transition: Determination of $T_g = T_g(P)$, and the corresponding hole fraction at T_g: $h_g = h_g(P)$.
3. Glassy state: Determination of the hole fraction, $h = h(P, T)$, followed by calculation of the pressure dependence of the frozen free volume fraction, $FF = FF(P)$.

Molten State

The experimental data at $T > T_g$ were fitted to *S*–S EOS, using Scientist™ from MicroMath nonlinear least squares iterative fitting protocol. Rapid convergence was obtained in two-steps—fitting the data to the polynomial expression, $\tilde{V} = \tilde{V}(\tilde{P}, \tilde{T})$,[15] thus extracting the initial values of P^*, T^*, and V^* subsequently used to fit the data to eqs 6 and 7. Table 2 lists these parameters, along with the goodness of fit measures for specific volume, σ: standard deviation and r^2: correlation coefficient squared. Judging by the latter values, the *S*–S EOS well described the data. Similar good fits have been reported before.[16–20,23,25,58]

Table 2. The Characteristic Reducing Parameters and the Statistical Fit Data

No.	Polymer	P^* (bar)	T^* (K)	$10^4 \times V^*$ (mL/g)	M_s	σ	r^2	Ref.
1	PS-686	7139 ± 41	12811 ± 49	9630 ± 8	51.64	0.00045	0.9999998	15,34
2	PS-667	7741 ± 12	11736 ± 9	9516 ± 2	44.30	0.00068	0.9999995	60
3	PS-1301	7435 ± 26	11723 ± 22	9526 ± 5	45.87	0.00111	0.9999987	60
4	PS-Z110[a]	8044 ± 46	12256 ± 37	9581 ± 7	52.08	0.00097	0.9999990	TW[b]
5	PS-Z34[a]	8277 ± 34	12030 ± 34	9579 ± 5	52.07	0.00058	0.9999997	TW
6	PS-Z9[a]	8407 ± 33	11873 ± 25	9612 ± 5	52.06	0.00062	0.9999996	TW
7	PS-Z09	7759 ± 28	10050 ± 25	9839 ± 4	52.06	0.00101	0.9999990	60
8	PC	9521 ± 65	11986 ± 35	8167 ± 8	42.72	0.00089	0.9999990	TW
9	PPE-126C	8796 ± 106	10672 ± 60	8696 ± 20	38.67	0.00152	0.9999977	TW
10	PPE/PS	8323 ± 59	11668 ± 39	9155 ± 10	42.44	0.00127	0.9999984	TW

[a] Data recomputed for $3c = s$.
[b] TW indicates "this work."

Glass Transition

In this article T_g was determined only from the *PVT* plots. Thus, for systems of the type shown in Figure 1, T_g was taken as an intersection of the two straight lines ln V versus T at constant P, in melt and glass. For polymers with the transient zone **T** (see Fig. 2) T_g was taken at the boundary between the melt and the **T-**region. Using the characteristic reducing parameters of Table 2, the hole fraction at $T_g = T_g(P)$, $h_g = h_g(T_g, P_g)$, was computed from eqs 6 and 7. The values of T_g and h_g, at ambient pressure ($P = 1.0132$ bar), as well as their gradients dT_g/dP, dh_g/dP, and d^2h_g/dP^2 are listed in Table 3. Examples of the $T_g = T_g(P)$ and $h_g = h_g(P)$ dependencies are displayed in Figure 4.

Glassy State

From the *PVT* measurements at $T' < T_g$ one might calculate the hole fraction in the glass,[61] $h_{glass} = h(T', P')$, by substituting $V = V(T', P')$ into eq 6; evidently, the reducing parameters for the polymer (P^*, T^*, V^* determined from data at $T > T_g$) must be known (n.b., the independent variables in the glassy state are indicated by "prime," *viz.* T', and P'). The hole fraction that melt would have if existed under the conditions of T' and P', $h_{melt} = h(T', P')$, is readily computed from eqs 6 and 7 using the same P^*, T^*, V^*, with T' and P' as independent variables (an example is presented in Fig. 5). The isobaric values of h show significantly more free volume in the vitreous state than what it would be expected if the melt existed under these

Table 3. The Glass Transition Parameters and the Statistical Fit Data

No.	Polymer	T_g (K) at $P = 1.0132$ bar	dT_g/dP (K/kbar)	h_g (−) at $P = 1$ bar	dh_g/dP (1/Mbar)	d^2h_g/dP^2 (1/Gbar^2)	r[a]
1	PS-686[b]	368.4	74.1	0.0603	−14.8	+4.38	0.999
2	PS-667	361.0[c]	29.3	0.0687	−11.5	+1.54	0.977
3	PS-1301	365.0	35.4	0.0689	−2.48	+0.877	0.778
4	PS-Z110	367.2	33.9	0.0763	−14.9	+1.97	0.999
5	PS-Z-34	369.6	33.6	0.0832	−14.5	+2.17	0.999
6	PS-Z-9	365.4	28.9	0.0828	−13.9	+2.11	0.997
7	PS-Z-09	(302.1)[d]	24.2	0.0653	−12.1	+2.14	0.989
8	PC	416.7	40.2	0.0921	−8.35	+1.34	0.996
9	PPE	462.2	78.0	0.1417	−6.26	−1.40	0.997
10	PPE/PS	417.9	44.5	0.1007	−13.1	+0.724	0.996

[a] The correlation coefficient.
[b] Only low-P data used.
[c] PS-667 contains 700 ppm Zn-stearate and 2.5% of mineral oil.
[d] Extrapolated value from higher P.

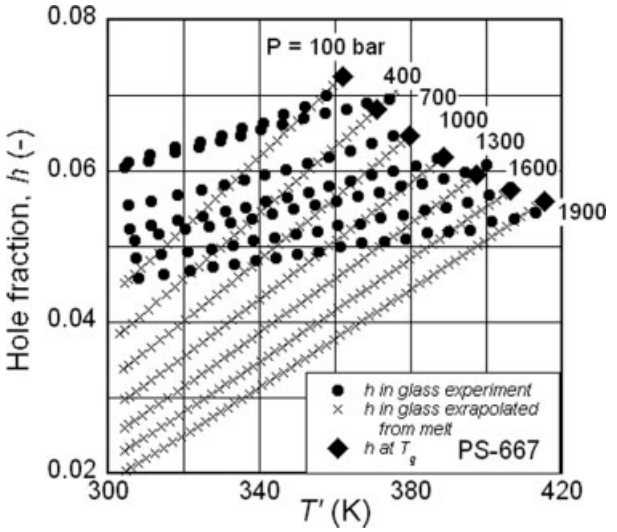

Figure 5. Isobaric temperature dependence of the hole fraction at $T' < T_g$ for PS-667; solid circles: hole fraction calculated from experiments; crosses: h extrapolated from the melt; solid diamonds: h at T_g. Test pressures are indicated.

conditions. From the h versus T isobaric dependencies in the glassy state and the extrapolated h-values from the melt to $T' < T_g$ the frozen fraction of free volume can be expressed as (Figs. 5–8):[55]

$$\left.\begin{aligned} FF_T &= 1 - \frac{(\partial h/\partial T')_{P,\text{glass}}}{(\partial h/\partial T')_{P,\text{melt}}} \\ FF_P &= 1 - \frac{(\partial h/\partial P')_{T,\text{glass}}}{(\partial h/\partial P')_{T,\text{melt}}} \end{aligned}\right\} FF_T = FF_P \qquad (9)$$

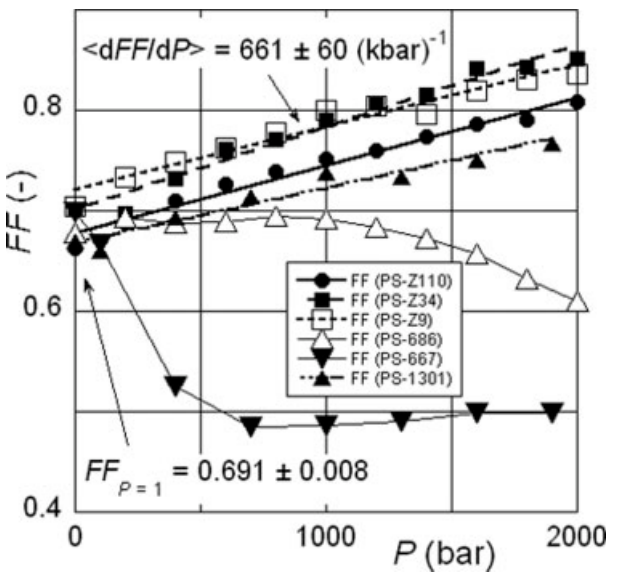

Figure 6. Pressure dependence of the free volume frozen fraction for six PS resins. At ambient pressure, the frozen fraction is $FF_{P=1} = 0.691 \pm 0.008$.

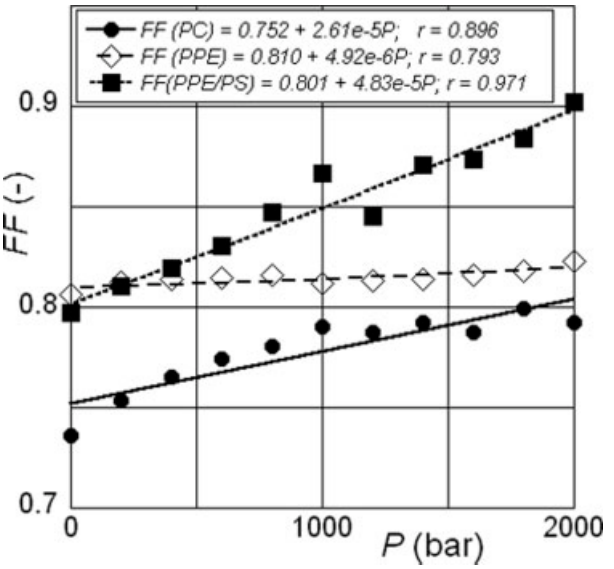

Figure 7. Pressure dependence of the frozen free volume fraction for the engineering resins: PC, PPE, and PPE/PS 1:1 blend.

To compute the derivatives $(\partial h/\partial T')_{P,\text{glass}}$, and $(\partial h/\partial T')_{P,\text{melt}}$, and then FF_T, an isobaric plot (e.g., see Fig. 5) might be used. In the case of PVT plots with large transient zone (see Fig. 2), only the glassy and molten regions are considered. For most polymers, the isobaric temperature depend-

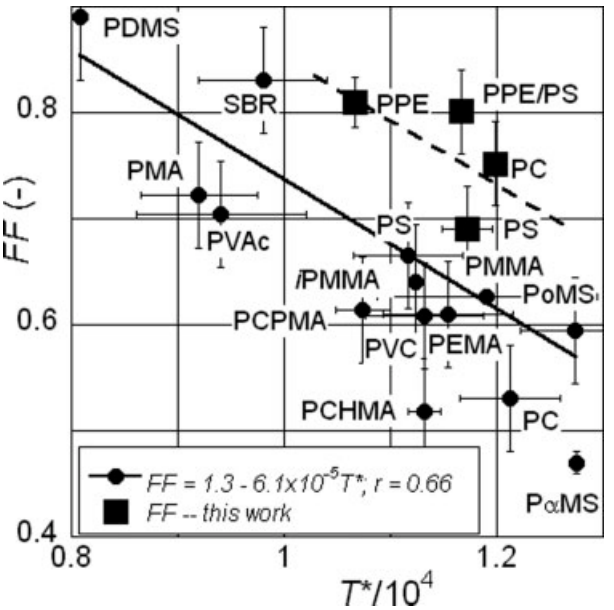

Figure 8. Frozen free volume fraction at ambient pressure (P = 1.0132 bar) versus the characteristic reducing temperature. Data from ref. 38 and this work.

ence of h within the glassy and molten zones is well approximated by straight lines with high correlation coefficient $r \geq 0.99$.

For poly(2,6-dimethyl 1,4 phenylene ether) (PPE) the β-transition takes place at $T_\beta \cong 367$ K, but it is not evident in the *PVT* plot. However, for the PPE/PS 1:1 blend, a transition is apparent at about 370 ± 5 K, and hence below the blend $T_g \cong 418$ K. The observed transition coincides with T_g of the PS component.

DISCUSSION

Molten State

As evident from the data in Table 2, *S*–S EOS well describes the *PVT* surface. For commercial high molecular weight (M_W) resins, where the number of statistical segments $s \gg 3$, the approximation $3c = s$ is quite reasonable. However, for oligomeric PS-Z09 (and to be consistent for other resins of the PS-Z type) originally the *PVT* data were fitted to *S*–S EOS, assuming linear variation of the flexibility ratio:[58]

$$3c/s = 1 + 3/s \tag{10}$$

The computations yielded $3c/s = 1.161$–1.427 for PS-Z110–PS-Z09, respectively. For PS-Z110, where $s \cong 2000$, eq 10 predicts $3c/s = 1.0015$ instead of the computed value of 1.161. Thus, the nonlinear, iterative least squares fitting method treats the flexibility parameter $3c/s$, as an additional adjustable variable for the optimization of data fit to eqs 6, 7, and 10.

It is noteworthy that the flexibility parameter, $3c/s$, enters the *S*–S EOS only through eq 7, which is not valid in the glassy, nonequilibrium state. When eq 6 is used to compute the free volume parameter h in the glassy region the procedure implies assumption that $3c/s = 1$.[34,55,56,62] As a consequence, computing h in the melt from eqs 6, 7, and 10 and that in the glass from eq 6 creates a discontinuity of the $h = h(P, T)$ function at T_g, and inconsistent values of *FF*. For this reason, the *PVT* data of PS-Z type in the molten state were recomputed assuming $3c/s = 1$, what induced relatively small changes in the precision of data fitting and the computed parameters. For example, the standard deviations for specific volume of PS-Z110, PS-Z34, and PS-Z9, computed with adjustable $3c/s$ were $\sigma = 0.00085$, 0.00056, and 0.00056, respectively, instead of $\sigma = 0.00097$, 0.00058, and 0.00062 in Table 2, obtained assuming that $3c = s$. The table also lists the P^*, T^*, V^* values obtained by fitting the *S*–S EOS (with $3c = s$). These quantities related to the volume-averaged Lennard-Jones parameters, ε^* and v^* through eq 4:

$$\varepsilon^* \cong RT^*/30 = 2.7715T^*(\text{J/mol}); \quad \text{and } v^* = V^*M_s(\text{mL/mol}). \tag{4a}$$

As reported earlier,[58] ε^* increases with log M_w (chain-end effect), and it is affected by chain configuration and additives. Furthermore, linear correlation between ε^* and v^* was found. Similar tendencies are also valid for the present set of data. Considering the limited number of studied polymers, the interaction parameters for PS can be represented by the averages $\varepsilon^* = 32.7 \pm 0.9$ (kJ/mol) and $v^* = 48.1 \pm 1.4$ (mL/mol). For PC $\varepsilon^* = 33.2$, $v^* = 34.9$ and for PPE $\varepsilon^* = 29.6$, $v^* = 33.6$, were calculated with the experimental uncertainty of 1.2 and 3.8%, respectively. The new set of the interaction parameters for PS confirms the previous findings. However, most interesting is the low value of v^* for PC (bisphenol-A polycarbonate) and PPE, which most likely reflects the main-chain flexibility engendered by the presence of the oxygen atom.[63]

In recent years, molecular modeling and the dynamic scattering experiments greatly improved understanding of the liquid structures at $T > T_g$, and their variability with temperature.[49–52] During cooling from high temperature to T_g, a liquid is affected by several dynamic events, which modify its macrobehavior. There has been significant progress in understanding of the liquid structures dependence on T, stemming mainly from the molecular modeling and neutron scattering experiments.[50,51]

An existence of the dynamic crossover has been demonstrated at $T > T_g$, and its existence interpreted by several mechanisms.[64] For example, the mode-coupling theory (MCT) considers a liquid as an assembly of particles enclosed in cages formed by their neighbors. During cooling from the liquid state, there are two relaxations—segmental (at $T > T_c$) and structural (at $T < T_c$). The crossover transition temperature, T_c, of these two takes place at about constant T_c/T_g ratio; for PS and PIB the event was observed at $T_c/T_g = 1.15$ and 1.35, respectively.[46] Two other relaxation processes the fast and the elementary complicate the structural changes. The former, which originates

is backbone chain vibrations or side groups motion, starts near the Vogel–Fulcher–Tammann–Hesse (VFTH) temperature in the glassy state and stretches to $T > T_c$. In macromolecular liquids the elementary relaxations are related to conformational transitions, which extend to temperatures well above T_c.[65,66]

Thus, at $T > T_g$ there are several relaxation processes. The crossover transition falls within the range of the so-called liquid–liquid transition temperature, $T_{LL}/T_g = 1.2 \pm 0.1$, described by Boyer as: "T_{LL} is a molecular level transition-relaxation associated with the thermal disruption of segment–segment contacts." Initially Boyer postulated that T_{LL} is a third order thermodynamic transition. This controversial idea was accepted by several researchers, while others suggested a dynamic nature,[67,68] or denied its existence.[69] The existence of a transition at $T > T_g$ has been reported for many glass-forming, fragile liquids.[68,70–72] As it will be discussed later, in spite of the apparent absence of any secondary transition on the *PVT* surface, the crossover temperature, $T_c \approx 1.2\ T_g$, is evident in $\kappa = \kappa(P, T)$ plots.

Glass Transition

To illustrate how T_g was determined, *PVT* behavior of two PS resins is displayed in Figures 1 and 2. The former figure (for PS-667) illustrates behavior of a specimen, taken from extrusion line, loaded into the Gnomix dilatometer and isobarically heated from the ambient temperature to 240 °C, then cooled back to room temperature, compressed to the next level of P, heated back to 240 °C, etc. The resulting *PVT* surface looks deceptively simple, and here T_g is defined by the change of slope of the ln V versus T relation. By contrast, the *PVT* graph of PS-686 in Figure 2 is more complex, showing a large transitory zone **T** between the glassy and molten regions. This resin was also measured isobarically but by cooling from $T \cong T_g + 30$ to ambient temperature, then reheating the specimen back to $T_g + 30$, increasing P and repeating the cooling cycle.[34,60] In this case, T_g is taken as the boundary temperature between the transitory and molten state.

Evidently, the character of h changes across the glass transition; while in the melt its equilibrium value depends only on P and T, in the glassy region it also depends on the way glass was prepared, and on time, for example, $y = 1 - h = y(P, T, t_a)$, where t_a is the annealing time. McKinney and Simha expressed the reduced pressure as a general function of $\tilde{T}, \tilde{V}, y$:[55,56]

$$-\tilde{P} = (\partial\tilde{F}/\partial\tilde{V})_{\tilde{T},y} + (\partial\tilde{F}/\partial y)_{\tilde{T},\tilde{V}}(\partial y/\partial\tilde{V})_{\tilde{T}} \quad (11)$$

where $\tilde{F}$ is the Helmholtz free energy in reduced variables. The derivatives in eq 11 were computed using iterative numerical method. At the thermodynamic equilibrium $(\partial F/\partial y)_{\tilde{T},\tilde{V}} = 0$, and eq 11 simplifies to the well-known definition of $\tilde{P}$.

The authors analyzed *PVT* data of PVAc by means of eq 11, as well as following the simplified procedure, that is, using eq 6 alone.[34,55,56,62,73] The two methods gave identical solution for $T \geq T_g$. In glass the difference between the h-values increased as T decreased. In consequence, the frozen fraction parameter, *FF*, computed from eq 11 was about 10% higher than that calculated using the simplified procedure (the experimental error of *FF* is about ±6%). Furthermore, all functions computed by these two methods showed similar tendencies. Thus, the use of the simplified procedure might be justified as the method offering a relatively rapid evaluation of polymer behavior in the glassy state.

Since T_g depends on the way the glass was prepared, the pressure dependence of T_g, dT_g/dP, is a function of the thermodynamic history. In analogy to the Ehrenfest derivation, formally setting $f(T, P, h) = 0$, one obtains P-derivative at T_g as:[34,55,56,62,78]

$$dT_g/dP = (\partial T/\partial P)_h + (\partial T/\partial h)_P(dh/dP) \cong \Delta\kappa/\Delta\alpha + (\partial T/\partial h)_P(dh/dP) \quad (12)$$

where $(\partial T/\partial h)_P$ is computed from the isobaric data in the molten state near T_g, using eqs 6 and 7, and $(dh/dP) = dh(T_g, P_g)/dP$ is calculated along the $T_g = T_g(P)$ line.

As shown in Figure 3, T_g and h_g at ambient pressure, $P \to 0$, are interrelated—the higher T_g the larger h_g. In the figure, the pressure effect on the dependence is also indicated by open squares; now the dependence is reversed—the higher T_g the smaller h_g. Rationalization of this reversal is obvious from data displayed in Figure 4; evidently the pressure reduction of h_g overpowers its increase with T_g.

Polymer vitrification might be achieved by isobaric cooling or by isothermal compression. Experimentally, the gradients of these two processes are related, $dT_g/dP \cong (dP_g/dT)^{-1}$, confirming that the derivatives are total.[35] Judging by the values of dT_g/dP in Table 3, the gradient depends on M_n, molecular polydispersity, type and amount of additives, but

mainly on the method and the rate of vitrification. As earlier studies demonstrated, PS-686 vitrified by isobaric cooling, and by isothermal compression showed $dT_g/dP = 74.2$ and 31.6 (1/kbar), respectively.[34] The dT_g/dP values listed by Roe range from 16 to 31 K/kbar.[75] The values obtained using the standard *PVT* test procedure fall within these ranges.

The shape to the $T_g = T_g(P)$ function also depends on the vitrification rate and method.[28] In the present studies, for most polymers the dependence was linear. However, for PS-Z110, PS-Z34, PPE-126, PS-686, and PPE/PS blend, the second order polynomial, $T_g = \Sigma a_i P^i$, had to be used with $10^6 \times a_2 = 3.93$, 2.64, 11.4, 4.60, and 6.81, respectively.

For the tested PS resins T_g varies with the number-averaged molecular weight (M_n) as:[76]

$$T_g = T_g^\infty - K/M_n \qquad (13)$$

Using the data from Tables 1 and 3, the equation parameters: $T_g^\infty = 370 \pm 1$ K, and $K = 53 \pm 2$ (kg/mol) were determined. While the former is comparable to the value published by Enns and Boyer,[77] or quoted by Bicerano,[52] *viz.* $T_g^\infty = 371$, and $T_g^\infty = 382$ K, respectively, the latter is quite different from their values, *viz.* $K = 116$, and 200 (kg/mol), respectively. Evidently, the difference originates in M_n—used in this work as reported by the manufacturers.

Considering the diversity of the method of vitrification used in the present study, it is desirable to compare the experimental values of dT_g/dP with those computed from the extended Ehrenfest-type dependence, eq 12. The comparison is time consuming, and since it involves α and κ derivatives, it is sensitive to experimental errors, presence of secondary transitions, as well as the methods of computation. For example, *S*–S EOS is well approximated by the polynomial expansion $\ln V = f(P, T)$,[15] but derivatives of the polynomial are significantly different from the values calculated directly from the experimental data. Similar disparities were obtained from curve fitting to others, more complex expressions, and then their differentiation. It is also worth recalling that careful analysis of *PVT* data of polymethacrylates detected sub-T_g transitions in a plot of $d\alpha_{glass}/dT$ versus T, but only for highly isotactic poly(methyl methacrylate) (I-PMMA).[38] The reason for the inconsistency is the dependence of κ (and α to a lesser extend) on P and T.

In consequence, the calculations were carried out directly from the isobaric plots on $\ln V$ versus T or from the isothermal ones of $\ln V$ versus P, scrutinizing in particular the expected transition regions, then fitting each set of experimental data to an appropriate order polynomial, and finally differentiating it. For all PS resins, the former plots were linear on both sides of T_g resulting in T-independent α-values, which slowly decreased with P. As an example, in Figure 9 the thermal expansion coefficient of PS-667 in the molten and glassy state is plotted versus P. The data are well described by the second order polynomials:

$$10^4\alpha_{melt} = 5.885 - 2.163 \times 10^{-3}P + 4.706 \times 10^{-7}P^2; r = 0.999$$

$$10^4\alpha_{glass} = 2.789 - 1.021 \times 10^{-3}P + 2.592 \times 10^{-7}P^2; r = 0.994$$

Variability of the compressibility coefficient, κ, is more serious, as in the glassy and molten state this parameter was found to depend on T and P. However, while in the vitreous state the dependence was monotonic (no sign of the β-transition), in the melt the behavior was complex (see Figures 10 and 11 for PS-686 and PS-Z110, respectively). For both resins, the isobaric κ is plotted versus T ($\geq T_g$). It is noteworthy that different dilatometers, operators, and test procedures have been used, *viz.* PS-686 was isobarically cooled, while PS-Z110 was isothermally compressed (the standard test procedure).[59] This indicates that the observed variability of κ is inherent. The compressibility coefficient, κ, becomes a linear function of T, only above 450 K. In other words, the compressibility linearly changes with T only above a crossover temperature. Its value at ambient pressure is $T_c \approx 1.23\, T_g$. Surprisingly, judging by the dependencies in Figures 10 and 11, this transition temperature seems to be insensitive to pressure.

The Ehrenfest eq 2 and its extended version, eq 12, assume that the vitrification is a second-order pseudoequilibrium process, neither the rate nor the vitrification method (cooling versus compression) is taken into account. The *FF* versus P dependencies of PS displayed in Figure 6 fall into three categories: (1) PS-686 cooled isobarically from $T \cong T_g + 30$, (2) PS-667 isothermally pressure scanned, and (3) the remaining four premolded resins (represented by PS-Z110) isothermally scanned following the standard *PVT* test procedure. In consequence, it is expected that PS-686 might follow eq 12, the resins of category (3) should not, and that PS-667 should show the greatest deviation. To be consistent with the *FF*

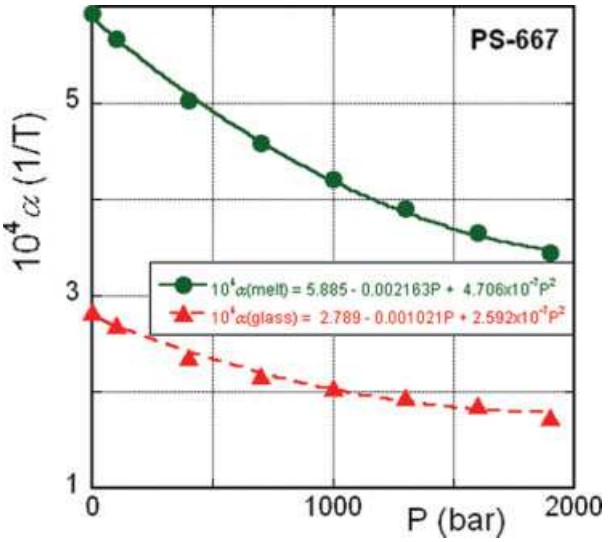

Figure 9. Pressure dependence of the thermal expansion coefficient, α, for PS-667 in the glassy and molten state.

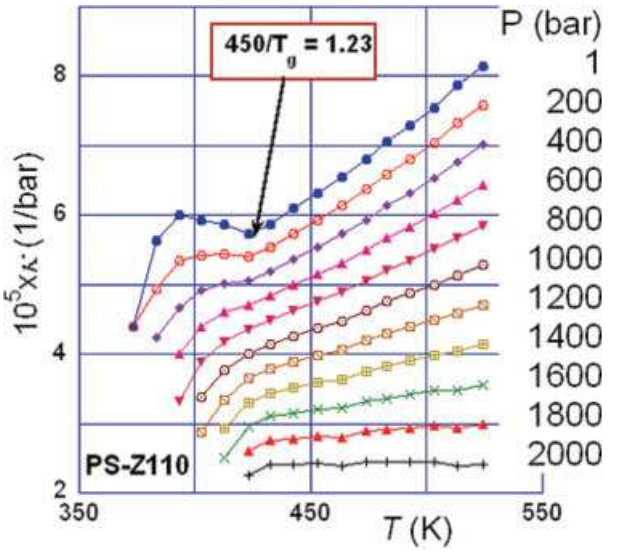

Figure 11. Temperature and pressure dependence of the compressibility coefficient, κ, for PS-Z110 in the molten state.

calculations, the derivatives in the molten state were taken in the immediate vicinity of T_g, while these in the glass near the temperature limiting the transition region (see Fig. 2).

Results of these computations are presented in Figure 12. For the three polymers, the direct derivative dT_g/dP shows relatively small variations: 39.1 ± 1.8, 26.0 ± 1.6, and 30.0 ± 1.6 (K/kbar) for PS-686, PS-667, and PS-Z110, respectively. For PS-686 the gradient computed from eq 12 slightly varies with P: dT_g/dP (calc) = 40.0 ± 2.7 (K/kbar), but at the same time it concords with the experimental value. The $\Delta\kappa/\Delta\alpha$ ratio for PS-686 is almost P-independent, $\Delta\kappa/\Delta\alpha$ = 55.5 ± 2.7, while that for the other resins shows strong P-dependence. The negative product of the other derivatives in eq 12 is relatively constant; thus it does not modify the P-effect on dT_g/dP (calc). As a result, the source of

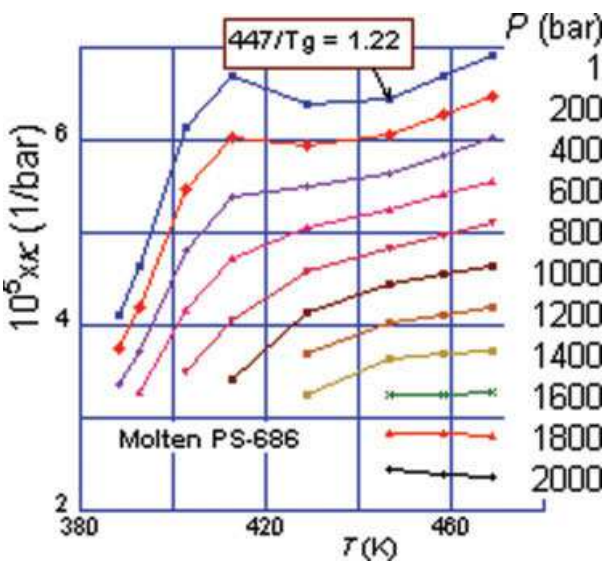

Figure 10. Temperature and pressure dependence of the compressibility coefficient, κ, for PS-686 in the molten state.

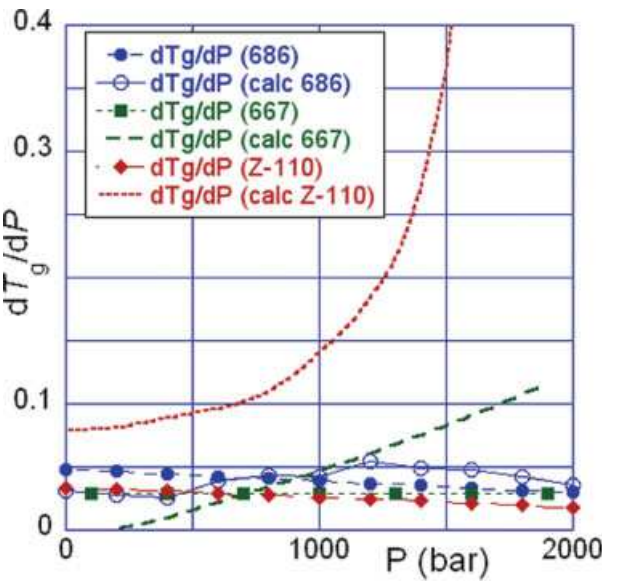

Figure 12. Pressure dependence of the T_g pressure gradient, dT_g/dP, for PS-686, PS-667, and PS-Z110; solid points are for the direct derivative, while lines were computed from eq 12.

disparity between the experimental and calculated dT_g/dP gradient evident in Figure 12 is the pressure dependence of $\Delta\kappa$, magnified by small (and decreasing with P) value of $\Delta\alpha$. For PS-1301 and the three PS-Z resins, this interpretation is in qualitative agreement with the large values of FF that increases with P (see Fig. 6).

Glassy State

The simplified method of analysis of the glassy state involves computing of h in the melt from eqs 6 and 7 with $3c = s$, and in glass from eq 6 alone. As discussed before, the use of this simplified method is justified on the basis of the previous analyses.[34,55,56,62,78]

Cooling or compressing molten amorphous polymer transforms it into glass, following the rate-dependent function: $T_g = T_g(q, P)$, or $T_g = T_g(q, T)$, respectively, which engenders a variety of structures and affects the free volume content and its functional dependencies within the glassy state, $h = h(P, T, t_a)$. In simple terms, fast quenched glass has more free volume than a slow cooled one. Since glass is not at thermodynamic equilibrium, at temperatures $T_\beta < T < T_g$ it slowly relaxes by what was labeled by Struik as "physical aging."[79] The relaxation is accompanied by progressive loss of free volume.

The free volume content decreases with time at a rate dependent on T. Evidently, the rate is zero at $T > T_g$. Also, as discussed by Struik, at $T < T_\beta$ the molecular motion is sufficiently slow for the physical aging rate also to be practically zero. Empirically, the rate reaches the maximum value at $T_{max}/T_g \approx 0.87 \pm 0.03$. The temperature range of the maximum aging rate plateau seems to be related to $\Delta T = T_g - T_\beta$; the larger the ΔT the wider the plateau, for example, since for PC $\Delta T = 275$ °C the maximum aging rate for this polymer occurs at a range of about 160 °C. Resulting from the loss of free volume, the polymer density increases and it becomes more rigid and brittle; it undergoes physical aging. The process is similar for all glasses—organic or not.[80]

From the *PVT* standpoint, the glassy region is characterized by a larger free volume content, which could be expected if the thermodynamic equilibrium was valid.[32,38,55,56,62,78] This phenomenon might be discussed in terms of the frozen free volume fraction, FF (see eq 10). Figures 6 and 7 illustrate the pressure effects on FF for PS and for the other polymers, respectively. The shape of these dependencies is affected by the method of glass formation as well as by the procedure used for the *PVT* measurements. It is interesting that for all PS resins at the ambient pressure a common value, $FF_{P=1} = 0.691 \pm 0.008$, was obtained.

Fundamentally, the procedure should start from a thermodynamic equilibrium state and achieve the glassy state along a well-defined route; hence one should start with liquid polymer and vitrify it either by isobaric cooling or isothermal compression. Only measurements of PS-686 approached this recommended procedure. As Figure 6 demonstrates, the isobarically cooled melt resulted in glass having nearly constant amount of the frozen free volume fraction, $FF = 0.688 \pm 0.002$ at $P \leq 1200$ bar. Only at pressures, $1200 < P \leq 2000$, FF decreased by 11% to $FF = 0.610$. Since the melt is expected to be at thermodynamic equilibrium, any reduction of the *FF* originates in a decrease of free volume in the glass. Thus, apparently the slow cooling used during the *PVT* measurements provided sufficient time for a small loss of free volume, that is, for accelerated physical aging.

The *PVT* measurements of PS-667 were also isobaric, but by heating specimens taken from the extrusion line. Once the highest temperature was reached, the specimen was cooled down to ambient temperature, and pressurized to the next P-level, before starting the next isobaric heating. The procedure provided greater opportunity for the initial reduction of free volume content within the glassy region. There is a significant difference between *FF* value calculated from the first run ($FF \cong 0.698$ at $P = 100$ bar) and those determined at $P \geq 400$ bar pressures: $FF = 0.497 \pm 0.006$.

The other polymers in Figures 6 and 7 were measured following the "standard" procedure, where premolded specimens are isothermally pressurized from the lowest T and P (usually ambient) to the highest. For these samples FF increases linearly with P: $\langle dFF/dP \rangle = 661 \pm 60$ (1/kbar). Thus, as the isothermal tests progress from the ambient conditions the frozen fraction of free volume systematically increases. The measurements start with glasses with poorly defined thermodynamic history that are expected to have diverse molecular structures and free volume contents. However, the data in Figures 6 and 7 show that the standard test procedure leads to consistent performance.

The glass transition temperature for the 50:50 blend of PPE/PS calculated from the Fox relation is T_g (calc) = 411 K, to be compared with T_g (experiment) = 418 K determined from *PVT*.[81] The difference of 7 °C is outside the experimental error,

and it might indicate residual immiscibility of PPE with PS, reported by several research groups.[73] Further evidence of the immiscibility is found at $T < T_g$. Of the 10 studied polymers, the PPE/PS blend is the only one that shows a secondary transition below its $T_g \cong 418$ K. The transition, at about 370 ± 5 K, coincides with T_g of the PS component. According to nuclear magnetic resonance (NMR) studies only ~30 wt % blend components are fully miscible, the rest existing as well-dispersed domains.[82] The presence of dispersed PS domains could account for transitions in $h = h(T)$ and $\kappa = \kappa(T)$ at $T < T_g$.

The vitrification procedure affects the polymer structure and mobility, which are evident in diverse material behaviors, of which *PVT* is but one.[28,79] The loss of segmental mobility translates into freezing of free volume; the data in Figures 6 and 7 indicate that $0.5 < FF < 0.9$; hence most of the free volume at T_g initially remains in the glass, slowly dissipating during the physical aging—the higher the value of *FF* the larger the physical aging effects.

The cluster model of glassy amorphous polymers at $T_\beta \leq T \leq T_g$ assumes the presence of a matrix and dispersed in it clusters consisting of collinear close-packed macromolecular segments. The cluster concentration depends on T, $\varphi_c = \lambda(1 - T/T_g)^\gamma$ (where λ and γ are equation parameters, both <1), thus they exist only in the glassy state and on heating fully disintegrates at T_g.[83] If the model is correct, different free volume content must exist in matrix and clusters. Aging increases the content of the latter domains up to quasiequilibrium level. The model relates the cluster content to aging and increasing brittleness under ambient pressure. The positron annihilation lifetime spectroscopy (PALS) leads to the conclusion that during physical aging the average free volume cavity size does not change, while their total number decreases.[84,85] Thus, the cluster may have smaller number of the free volume cavities than the matrix. It is noteworthy that recent analyses of PALS data strongly suggest that the cavity shape is better described as a cylinder or elongated prism than a sphere.[29,30]

The data displayed in Figure 6 might be regarded as reflecting the isobaric dV/dT dependence at $T < T_g$. It is expected that FF is either independent of P or decreasing with it; hence the slope should be constant or increase with P. However, it is difficult to imagine a mechanism that will cause the slopes to decrease at higher P. The two aforementioned theories offer possible explanation, *viz.* different compressibility of cavities in the cluster and matrix and/or different geometry of cavities at different pressures.

SUMMARY AND CONCLUSIONS

The *PVT* behavior of 10 polymers in the molten and glassy state was analyzed using the Simha–Somcynsky equation of state (EOS). The results might be summarized as follows:

1. The *S*–S EOS well describes the *PVT* behavior in the melt. The accuracy of specific volume fit was within ±0.0003 mL/g.
2. Three methods of *PVT* testing were used: (a) isobaric cooling from $T_g + 30$, (b) isobaric heating from the ambient T and P, and (c) isothermal compressing from the ambient T and P. The three methods resulted in different glass behaviors.
3. For most polymers the glass transition pressure gradient dT_g/dP was constant, ranging from 24 to 78 (K/kbar). The Ehrenfest-type of relation was found to be obeyed only by PS cooled isobarically from $T_g + 30$. The polymers vitrified by the two other methods (see 2.) showed strong P dependence of the computed gradient, absent in the experimental data.
4. Independently of the *PVT* test procedure, all PS resins showed similar value of the free volume frozen fraction at ambient P; $FF_{P=1} = 0.691 \pm 0.008$. By contrast, the P-dependence of *FF* varied with the method of measurements and vitrification.
5. The thermal expansion coefficient, α, in the molten and glassy system was found to be independent of T, and slowly decreasing with P.
6. The compressibility coefficient, κ, depended on both, T and P. In the molten state its isobaric dependence on T indicated that a regular behavior is obtained only at $T > T_c \cong 1.2\,T_g$.
7. Since the free volume content in glassy polymer affects its physical aging, dimensional stability, and mechanical performance, the information on *FF* might be used for the minimization of aging effects.

NOMENCLATURE

$3c$	The external, volume-dependent degrees of freedom per macromolecule
$3c/s$	The flexibility parameter

$\tilde{F}$	Helmholtz free energy in reduced variables
$FF_T = FF_P$	Isothermal and isobaric frozen free volume fraction
h	Free volume parameter in *S–S* EOS; $h = h(V, T)$
h_g	h-Value at T_g
$MB_{sB} = M_n/s$	Molecular weight of statistical segment
M_n, M_w	Number- and weight-average molecular weight
P^o	The glass formation pressure
P, P^*	Pressure and the characteristic pressure reducing parameter
q	Rate of vitrification by either cooling or compressing
r^2	Correlation coefficient squared
R	The gas constant
s	Number of statistical segments per macromolecule
T	Transition zone
T^0	The glass formation temperature
T_0	Vogel–Tammann–Fulcher temperature
t_a	Annealing time
T_β	Beta or the subglass transition temperature
T_c	Crossover transition temperature, $T_c/T_g = 1.15$ to 1.35
T_g, T_g^∞	Glass transition temperature and its value at very high M_w
T_K	Kauzmann zero-entropy temperature, $T_K \approx T_g - 50$ K
T_{LL}	Liquid–liquid transition temperature, $T_{LL}/T_g = 1.2 \pm 0.1$
T_m	Melting point
T_{max}	Temperature at which the physical aging rate is the highest
T, T^*	Temperature and the characteristic temperature reducing parameter
v^*	L-J segmental repulsion volume per statistical segment
V, V^*	Specific volume and the characteristic volume reducing parameter
y	Occupied volume fraction in *S–S* EOS; $h = 1 - y$
$z = 12$	Coordination number
zq	The number of interchain contacts in a lattice $zq = s(z - 2) + 2$.
α	Thermal expansion coefficient
Δ	Difference between values for the liquid (l) and glassy state (g)
Δt_{max}	Delay time to reach the peak temperature in flammability tests
ε^*	L-J maximum attractive energy
η	Viscosity
κ	Compressibility
φ	Cluster concentration
σ	Standard deviation

Independent variables in the glassy state are indicated by "prime," *viz.* T', and P'.

Tilde indicates reduced variables, for example, as defined in eq 4.

The author thanks R. Simha for the numerous and fruitful discussions, as well as his comments and corrections of the manuscript.

REFERENCES AND NOTES

1. (a) Prigogine, I.; Trappeniers, N.; Mathot, V. Discuss Faraday Soc 1953, 15, 93; (b) Prigogine, I.; Trappeniers, N.; Mathot, V. J Chem Phys 1953, 21, 559.
2. Prigogine, I.; Bellemans, A.; Mathot, V. The Molecular Theory of Solutions; Amsterdam: North-Holland; 1957.
3. Flory, P. J.; Orwoll, R. A.; Vrij, A. J Am Chem Soc 1964, 86, 3567.
4. (a) Simha, R.; Somcynsky, T. Macromolecules 1969, 2, 342; (b) Somcynsky, T.; Simha, R. J Appl Phys 1971, 42, 4545.
5. Sanchez, I. C.; Lacombe, R. H. J Phys Chem 1976, 80, 2353.
6. Hartmann, B.; Haque, M. A. J Appl Polym Sci 1985, 30, 1553.
7. Dee, G. T.; Walsh, D. J. Macromolecules 1988, 21, 811, 815.
8. Ougizawa, T.; Dee, G. T.; Walsh, D. J. Polymer 1989, 30, 1675.
9. Tait, P. G. Phys Chem 1888, 2, 1.
10. Curro, J. G. J Macromol Sci Rev Macromol Chem Phys 1974, C11, 321.
11. Zoller, P.; In Polymer Handbook, 3rd ed.; Brandrup, J.; Immergut, E. H., Eds.; Wiley: New York, 1989, p VI/475.
12. Rodgers, P. A. J Appl Polym Sci 1993, 50, 1061.
13. Rudolf, B.; Kressler, J.; Shimomami, K.; Ougizawa, T.; Inoue, T. Acta Polym 1995, 46, 312.
14. (a) Simha, R.; Jain, R. K.; Jain, S. C. Polym Compos 1984, 5, 3; (b) Papazoglou, E.; Simha, R.; Maurer, F. H. J Rheol Acta 1989, 28, 302.
15. Utracki, L. A.; Simha, R. Macromol Theory Simul 2001, 10, 17.
16. (a) Simha, R.; Utracki, L. A.; Garcia-Rejon, A. Compos Interfaces 2001, 8, 345; (b) Utracki, L. A.; Simha, R.; Garcia-Rejon, A. Macromolecules 2003, 36, 2114.
17. Tanoue, S.; Utracki, L. A.; Garcia-Rejon, A.; Tatibouët, J.; Cole, K. C.; Kamal, M. R. Polym Eng Sci 2004, 44, 1046.
18. Utracki, L. A.; Simha, R. Macromolecules 2004, 37, 10123.

19. Utracki, L. A.; Simha, R. Polym Int 2004, 53, 279.
20. Utracki, L. A. J Polym Sci Part B: Polym Phys 2004, 42, 2909.
21. Curro, J. G.; Lagasse, R. R.; Simha, R. Macromolecules 1982, 15, 1621.
22. Utracki, L. A. J Rheol 1986, 30, 829.
23. Utracki, L. A.; Simha, R. J Polym Sci Part B: Polym Phys 2001, 39, 342.
24. Sedlacek, T. Int Polym Process 2005, 20, 286.
25. Utracki, L. A.; Sedlacek, T. Rheol Acta, in press.
26. Yu, Z.; Yahsi, U.; McGervey, J. D.; Jamieson, A. M.; Simha, R. J Polym Sci Part B: Polym Phys 1994, 32, 2637.
27. Higuchi, H.; Yu, Z.; Jamieson, A. M.; Simha, R.; McGervey, J. D. J Polym Sci Part B: Polym Phys 1995, 33, 2295.
28. Schmidt, M. Macroscopic Volume and Free Volume of Polymer Blends and Pressure-Densified Polymers. Ph.D. Thesis, Chalmers University, Göteborg, 2000.
29. Olson, B. G. Positron Annihilation Lifetime Studies of Polymers. Ph.D. Thesis, Case Western Reserve University, Cleveland, OH, 2004.
30. Consolati, G.; Quasso, F.; Simha, R.; Olson, B. G. J Polym Sci Part B: Polym Phys 2005, 43, 2225.
31. Dlubek, G.; Hassan, E. M.; Krause-Rehberg, R.; Pionteck, J. Phys Rev E 2006, 73, 031803.
32. McKinney, J. E. Ann NY Acad Sci 1976, 279, 88.
33. Nieuwenhuizen, Th. M. J Phys: Condens Matter 2000, 12, 6543.
34. Quach, A.; Simha, R. J Appl Phys 1971, 42, 4592.
35. Briatico-Vangosa, F.; Rink, M. J Polym Sci Part B: Polym Phys 2005, 43, 1904.
36. Arora, R. K.; Jain, R. K.; Nanda, V. S. J Polym Sci Part B: Polym Phys 2001, 39, 515.
37. (a) Lennard-Jones, J. E. In Statistical Mechanics; Fowler, R. H., Ed.; Cambridge University Press: Cambridge, 1929, Ch. X; (b) Lennard-Jones, J. E. Proc Phys Soc London 1931, 43, 461; (c) Lennard-Jones, J. E.; Devonshire, A. F. Proc R Soc London 1937, 163, 53.
38. (a) Wilson, P. S.; Simha, R. Macromolecules 1973, 6, 902; (b) Simha, R.; Wilson, P. S. Macromolecules 1973, 6, 908.
39. Sachdev, V. K.; Jain, R. K. J Polym Sci Part B: Polym Phys 2005, 43, 1618.
40. (a) Boyer, R. F. In Encyclopedia of Polymer Science and Technology; Mark, H. F., Ed.; Wiley: New York, 1977; Vol. 2, pp 745–839; (b) Boyer, R. F. J Macromol Sci Phys 1980, 18, 461; (c) Boyer, R. F. In Order in the Amorphous State; Miller, R. L.; Rieke, J. K., Eds.; Plenum: New York, 1987, pp 135–185; (d) Boyer, R. F. In Polymer Yearbook, Vol. 2; Pethrick, R. A., Ed.; Harwood Academic Publishers: New York, 1985, pp 233–343.
41. Kozlov, G. V.; Beloshenko, V. A.; Varyukhin, V. N.; Lipatov, Yu. S. Polymer 1999, 40, 1045.
42. Bershtein, V. A.; Yegorov, V. M. Polym Sci USSR 1985, 27, 2743.
43. Baccaredda, M.; Butta, E.; Frosini, V.; De Petris, S. Mater Sci Eng 1968/69, 3, 157.
44. Etienne, S.; Lamorlette, C.; David, L. J Non-Cryst Solids 1998, 235/237, 628.
45. Pochan, J. M.; Pochan, D. F. Polymer 1991, 32, 2238.
46. Kisliuk, A.; Mathers, R. T.; Sokolov, A. P. J Polym Sci Part B: Polym Phys 2000, 38, 2785.
47. Bendler, J. T.; Fontanella, J. J.; Shlesinger, M. F.; Bartoš, J.; Šauša, O.; Krištiak, J. Phys Rev E 2005, 71, 031508.
48. Cowie, J. M. G.; McEwen, I. J.; McIntyre, R. In Polymer Blends Handbook; Utracki, L. A., Ed.; Kluwer: Dordrecht, 2002, Ch. 14.
49. Jackle, J. Rep Prog Phys 1986, 49, 171.
50. Kanaya, T.; Kaji, K. Adv Polym Sci 2001, 154, 87.
51. Binder, K.; Baschnagel, J.; Paul, W. Prog Polym Sci 2003, 28, 115.
52. Bicerano, J. In Encyclopedia of Polymer Science and Technology, 3rd ed.; Mark, H. F., Ed.; Wiley: Hoboken, NJ, 2003, p 655.
53. Kauzmann, W. Chem Rev 1948, 43, 219.
54. Gee, G. Polymer 1966, 7, 177.
55. McKinney, J. E.; Simha, R. Macromolecules 1974, 7, 894.
56. McKinney, J. E.; Simha, R. Macromolecules 1976, 9, 430.
57. Lee, W. A.; Knight, G. J. Br Polym J 1970, 2, 73.
58. Hartmann, B.; Simha, R.; Berger, A. E. J Appl Polym Sci 1989, 37, 2603.
59. Zoller, P.; Walsh, D. Standard Pressure-Volume-Temperature Data for Polymers; Technomic Publication: Lancaster-Basel, 1995.
60. Utracki, L. A. Polymer 2005, 46, 11548.
61. Quach, A.; Simha, R. J Phys Chem 1972, 76, 416.
62. Curro, J. G.; Lagasse, R. R.; Simha, R. J Appl Phys 1981, 52, 5892.
63. Flory, P. J. Statistical Mechanics of Chain Molecules; Interscience: New York, 1969;Chapter V.
64. Casalini, R.; Roland, C. M. Phys Rev B 2005, 71, 014210.
65. Ngai, K. L. J Non-Cryst Solids 2000, 275, 7.
66. Ngai, K. L. J Phys Condens Matter 2003, 15, S1107.
67. Patterson, G. D.; Bair, H. E.; Tonelli, A. E. J Polym Sci Polym Symp 1976, 54, 249.
68. (a) Murthy, S. S. N. J Mol Liq 1990, 44, 211; (b) Murthy, S. S. N. J Polym Sci Part B: Polym Phys 1993, 31, 475; (c) Murthy, S. S. N.; Kumar, D. J Chem Soc Faraday Trans 1993, 89, 2423.
69. Plazek, D. J. J Polym Sci Part B: Polym Phys 1982, 20, 1533.
70. (a) Angell, C. A. In Relaxation in Complex Systems; Ngai, K. L.; Wright, G. B., Eds.; NRL: Washington, DC, 1985, p 203; (b) Angell, C. A. Science 1995, 267, 1924; (c) Böhmer, R.; Ngai, K. L.; Angell, C.; Plazek, D. J. J Chem Phys 1993, 99, 4201.

71. Rao, K. J.; Bhat, M. H.; Kumar, S. J Indian Inst Sci 2001, 81, 3.
72. Buhot, A.; Garrahan, J. P. J Phys Condens Matter 2002, 14, 1499.
73. Utracki, L. A. Commercial Polymer Blends.Chapman & Hall: London, 1998.
74. Simha, R. Macromolecules 1977, 10, 1025.
75. Roe, R.-J. In Encyclopedia of Polymer Science and Technology, 2nd ed.; Mark, H. F., Ed.; Wiley: New York, 1987; Vol. 7, pp 531–544.
76. Fox, T. G.; Flory, P. J. J Appl Phys 1950, 21, 581.
77. Enns, J. B.; Boyer, R. F. In Order in Amorphous "State" of Polymers; Keinath, S. E.; Miller, R. L.; Rieke, J. K., Eds.; Plenum: New York, 1987, pp 221–249.
78. McKinney, J. E.; Simha, R. J Res Natl Bur Stand Sect A 1977, 81, 283.
79. Struik, L. C. E. Physical Aging in Amorphous Polymers and Other Materials; Elsevier: Amsterdam, 1978.
80. Matsuoka, S. J Res Natl Inst Stand Technol 1997, 102, 213.
81. Fox, T. G. Bull Am Phys Soc 1956, 1, 123.
82. Takahashi, H.; Inoue, Y.; Kamigaito, O.; Osaki, K. Kobunshi Ronbunshu 1990, 47, 611.
83. Kozlov, G. V.; Dolbin, I. V.; Zaikov, G. E. Russ J Appl Chem 2004, 77, 267.
84. Cangialosi, D.; Schut, H.; van Veen, A.; Picken, S. J. Macromolecules 2003, 36, 142.
85. Cangialosi, D.; Wübbenhorst, M.; Schut, H.; Picken, S. J. Acta Phys Polonica A 2005, 107, 690.